AD-A133 218 ANALYSIS OF LOW FREQUENCY GROUND MOTIONS INDUCED BY NEAR-SURFACE AND ATMO.. (U) S-CUBED LA JOLLA CA J R MURPHY ET AL. 01 AUG 82 SSS-R-82-5679 DNA-TR-81-157 1/1

UNCLASSIFIED DNA001-81-C-0215 F/G 18/3 NL

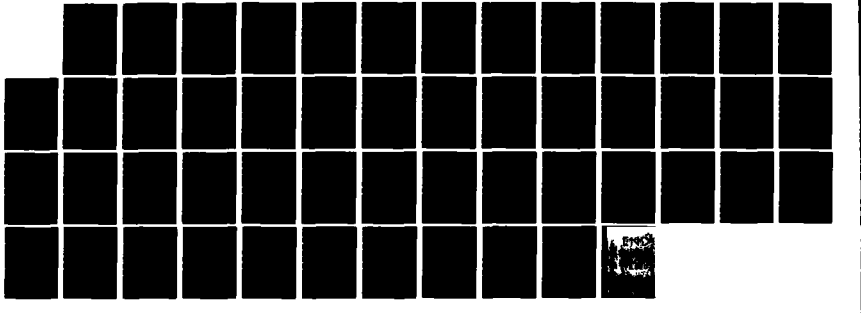

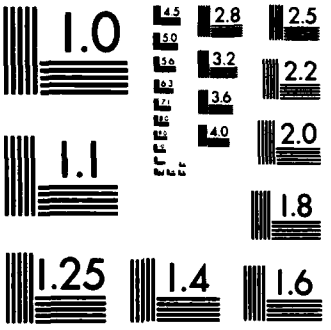

MICROCOPY RESOLUTION TEST CHART
NATIONAL BUREAU OF STANDARDS-1963-A

(12)

DNA-TR-81-157

ANALYSIS OF LOW FREQUENCY GROUND MOTIONS INDUCED BY NEAR-SURFACE AND ATMOSPHERIC EXPLOSIONS

J. R. Murphy
H. K. Shah
T. K. Tzeng
S-CUBED
P.O. Box 1620
La Jolla, California 92038

1 August 1982

Technical Report

CONTRACT No. DNA 001-81-C-0215

THIS WORK WAS SPONSORED BY THE DEFENSE NUCLEAR AGENCY
UNDER RDT&E RMSS CODE B344081466 Y99QAXSB00012 H2590D.

Prepared for
Director
DEFENSE NUCLEAR AGENCY
Washington, DC 20305

Destroy this report when it is no longer needed. Do not return to sender.

PLEASE NOTIFY THE DEFENSE NUCLEAR AGENCY, ATTN: STTI, WASHINGTON, D.C. 20305, IF YOUR ADDRESS IS INCORRECT, IF YOU WISH TO BE DELETED FROM THE DISTRIBUTION LIST, OR IF THE ADDRESSEE IS NO LONGER EMPLOYED BY YOUR ORGANIZATION.

UNCLASSIFIED

SECURITY CLASSIFICATION OF THIS PAGE (When Data Entered)

REPORT DOCUMENTATION PAGE		READ INSTRUCTIONS BEFORE COMPLETING FORM
1. REPORT NUMBER DNA-TR-81-157	2. GOVT ACCESSION NO. AD-A133 218	3. RECIPIENT'S CATALOG NUMBER
4. TITLE (and Subtitle) ANALYSIS OF LOW FREQUENCY GROUND MOTIONS INDUCED BY NEAR-SURFACE AND ATMOSPHERIC EXPLOSIONS		5. TYPE OF REPORT & PERIOD COVERED Technical Report 6. PERFORMING ORG. REPORT NUMBER SSS-R-82-5679
7. AUTHOR(s) J. R. Murphy H. K. Shah T. K. Tzeng		8. CONTRACT OR GRANT NUMBER(s) DNA 001-81-C-0215
9. PERFORMING ORGANIZATION NAME AND ADDRESS S-CUBED P. O. Box 1620 La Jolla, California 92038		10. PROGRAM ELEMENT, PROJECT, TASK AREA & WORK UNIT NUMBERS Task Y99QAXSB-00012
11. CONTROLLING OFFICE NAME AND ADDRESS Director Defense Nuclear Agency Washington, D.C. 20305		12. REPORT DATE 1 August 1982 13. NUMBER OF PAGES 48
14. MONITORING AGENCY NAME & ADDRESS(if different from Controlling Office)		15. SECURITY CLASS. (of this report) UNCLASSIFIED 15a. DECLASSIFICATION/DOWNGRADING N/A

16. DISTRIBUTION STATEMENT (of this Report)

Approved for public release; distribution unlimited.

17. DISTRIBUTION STATEMENT (of the abstract entered in Block 20, if different from Report)

18. SUPPLEMENTARY NOTES

This work was sponsored by the Defense Nuclear Agency under RDT&E RMSS Code B344081466 Y99QAXSB00012 H2590D.

19. KEY WORDS (Continue on reverse side if necessary and identify by block number)

LOW FREQUENCY	EXPLOSION
GROUND MOTION	HEIGHT OF BURST
RAYLEIGH WAVES	PRE-DIRECT COURSE

20. ABSTRACT (Continue on reverse side if necessary and identify by block number)

This report describes the results of a preliminary analysis of the effects of variations in height of burst (HOB) on the low frequency ground motions induced by near-surface and atmospheric explosions. A mathematical model which can be used to simulate this component of the explosively generated ground motions is described and applied to the parametric investigation

- continued -

DD FORM 1 JAN 73 1473 EDITION OF 1 NOV 65 IS OBSOLETE

UNCLASSIFIED

SECURITY CLASSIFICATION OF THIS PAGE (When Data Entered)

20. ABSTRACT (Continued)
of the effects of HOB on a prototype 1 kt nuclear explosion detonated over a site model approximating the subsurface geology at Yucca Flat on the Nevada Test Site. These simulations indicate that although the details of the airblast loading vary considerably with HOB, the corresponding induced low frequency Rayleigh waves are essentially independent of HOB for HOB ranging from 0 to 500 m, at least for this site.

The same theoretical model is also applied to the simulation of the low frequency ground motions to be expected from the proposed Pre-Direct Course HE experiment and a hypothetical surface burst test of the same yield at that site. It is shown that the surface waves predicted on the basis of the currently available subsurface model of the site are quite simple and pulse-like and also show little dependence on HOB over the range considered.

TABLE OF CONTENTS

Section		Page
I	INTRODUCTION	5
II	RAYLEIGH WAVES FROM NEAR-SURFACE AND ATMOSPHERIC EXPLOSIONS	7
	2.1 Model Definition.	7
	2.2 Airblast Loading From Atmospheric Explosions.	9
	2.3 Simulated Rayleigh Waves From Explosions With Different HOB.	20
III	APPLICATION TO THE PRE-DIRECT COURSE EXPERIMENT	30
IV	SUMMARY AND CONCLUSIONS.	38
	4.1 Summary	38
	4.2 Conclusions	39
	REFERENCES	41

LIST OF ILLUSTRATIONS

Figure		Page
1	Multilayered elastic halfspace loaded by a surface overpressure	8
2	Schematic illustration of overpressure time history predicted by the Speicher and Brode (1981) approximation	10
3	Peak incident pressure as a function of range and HOB, W = 1 kt.	12
4	Shock arrival time t_a (left) and positive phase duration D_p (right) as a function of range and HOB, W = 1 kt.	13
5	Overpressure time histories as a function of HOB at a range of 100 m, W = 1 kt.	14
6	Overpressure time histories as a function of HOB at a range of 1000 m, W = 1 kt	15
7	Total impulse delivered to the ground within 2 km of ground zero as a function of HOB, W = 1 kt	17
8	Subsurface geologic model for Yucca Flat simulations.	21
9	Fundamental mode Rayleigh wave dispersion curves for Yucca Flat model.	22
10	Rayleigh wave site response function for Yucca Flat model	23
11	Comparison of Rayleigh wave displacement spectra as a function of HOB at a range of 2500 m, Yucca Flat, W = 1 kt	25
12	Vertical component Rayleigh wave displacements as a function of HOB at a range of 500 m, Yucca Flat, W = 1 kt	26
13	Vertical component Rayleigh wave displacements as a function of HOB at a range of 1000 m, Yucca Flat, W = 1 kt	27
14	Vertical component Rayleigh wave displacements as a function of HOB at a range of 2500 m, Yucca Flat, W = 1 kt	28

LIST OF ILLUSTRATIONS (CONT'D)

Figure		Page
15	Subsurface geologic model and associated fundamental mode Rayleigh wave dispersion curves, Pre-Direct Course	31
16	Pre-Direct Course Rayleigh wave site response function (A_R).	32
17	Comparison of peak overpressures as a function of range for Pre-Direct Course and a surface burst test of the same yield.	34
18	Predicted vertical component Rayleigh wave displacement as a function of range, Pre-Direct Course	35
19	Comparison of predicted vertical component Rayleigh wave displacements for Pre-Direct Course and a surface burst test of the same yield	37

I. INTRODUCTION

The estimation of the characteristics of the ground motions induced by near-surface and atmospheric explosions is a complex problem which has received extensive study for more than two decades. A complete solution to this problem would incorporate an explicit consideration of the highly nonlinear response of the medium in the immediate vicinity of ground zero, including the vaporization and crushing of the earth material, leading to the formation of a surface crater, and the subsequent radiation of seismic energy away from the central source region. While such a complete solution has not yet been successfully demonstrated, it has recently been shown (Murphy, 1978; Auld and Murphy, 1979; Murphy and Bennett, 1980) that, despite these complications, a significant portion of the ground motion induced by surface explosions can be explained using some simple linear, elastic approximations. In particular, it has been concluded that the late-time, low-frequency ground motions observed from such explosions are predominantly elastic Rayleigh waves produced by the airblast loading acting on the surface outside the region of strong nonlinear response. The significance of this finding with regard to prediction lies in the fact that the theory governing the generation and propagation of elastic Rayleigh waves is well developed and thus can be used to help define scaling laws for the low frequency components of the ground motion environments produced by near-surface explosions.

The research summarized in this report has focused on the extension of these results to include consideration of atmospheric explosions detonated over a wide range of height of burst (HOB). It is well known (*e.g.*, Brode, 1968) that the airblast associated with HOB explosions differs in many respects from that associated with surface explosions of the same yield. However, up until now, no systematic study has been made of how this variation of the airblast loading

function with HOB can be expected to affect the airblast-induced, low frequency components of the ground motion. An analytical and numerical procedure for estimating the low frequency ground motions produced by HOB explosions is described in Section II where the results of a sample parametric application to a model approximating the subsurface geology at Yucca Flat on the Nevada Test Site is also presented. In Section III, the model is applied to the prediction of the low frequency ground motions to be expected from the Pre-Direct Course high explosive experiment scheduled to be conducted at the White Sands Test Site in the fall of 1982. This is followed in Section IV by a summary, together with a statement of conclusions regarding the current state of knowledge with respect to these issues.

II. RAYLEIGH WAVES FROM NEAR-SURFACE AND ATMOSPHERIC EXPLOSIONS

2.1 MODEL DEFINITION

Research conducted over the past several years has provided strong evidence that the low frequency components of the ground motions produced by near-surface explosions are predominantly elastic Rayleigh waves driven by the airblast load acting on the surface outside the region where strong nonlinear effects occur (Murphy and Bennett, 1980; Murphy, 1981). Thus, the boundary value problem of interest for predicting these low frequency ground motion components focuses on estimation of the elastic response of a multilayered model of the subsurface site geology to a propagating normal load acting on the surface (*i.e.*, an approximation to an airblast). The geometry of the problem is illustrated in Figure 1 which shows a vertical section consisting of an axisymmetric sequence of constant thickness (d_i) layers overlying a semi-infinite halfspace being acted on by a concentrated surface source. As a first approximation, the layers are taken to be perfectly elastic and are characterized by their Lamé constants (λ,μ) and density (ρ). Assuming an axisymmetric airblast load, the Fourier transform of the Rayleigh wave component of the displacement for a particular mode at observation point $\tilde{r}$, $W(\omega,\tilde{r})$, can be written as a spatial integration over the Fourier transform of the overpressure, $p(r,\omega)$, in the form (Murphy and Bennett, 1980):

$$W(\omega,\tilde{r}) = -i\pi A_R(\omega) \left[H_0^{(2)}(k\tilde{r}) \int_{r_0}^{\tilde{r}} p(r',\omega)\, J_0(kr')\, r'\, dr' + J_0(k\tilde{r}) \int_{\tilde{r}}^{\infty} p(r',\omega)\, H_0^{(2)}(kr')\, r'\, dr' \right] \quad (1)$$

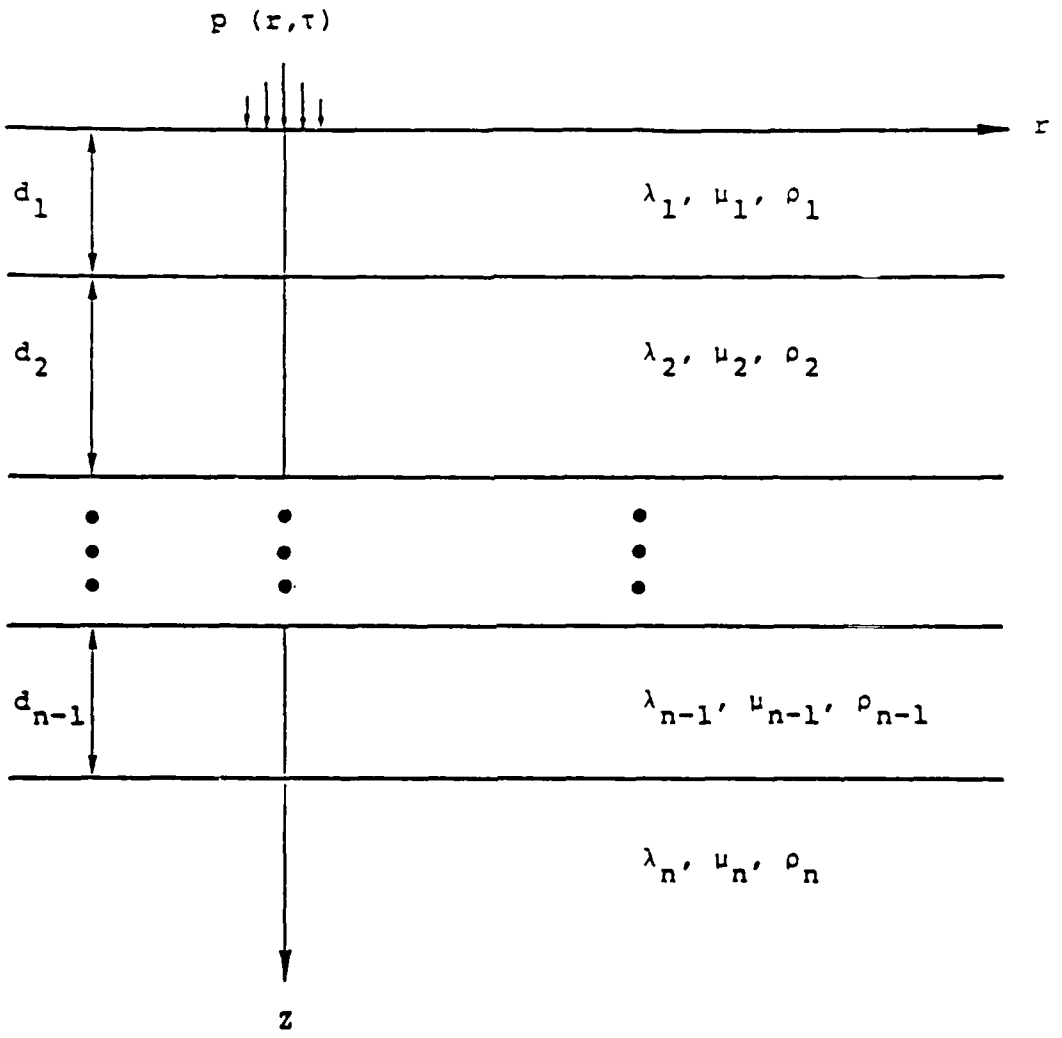

Figure 1. Multilayered elastic halfspace loaded by a surface overpressure.

where $A_R(\omega)$ is the Rayleigh wave site response function, J_0, $H_0^{(2)}$ denote the Bessel and Hankel functions respectively, k is the wavenumber of the Rayleigh wave component with frequency ω and r_0 denotes the exclusion radius which defines the region within which strong nonlinear effects occur. For surface bursts, it has been empirically determined that r_0 coincides approximately with the crater radius. However, for atmospheric explosions with significant HOB (*i.e.*, greater than r_0), it seems likely that this heuristic approximation can be avoided and r_0 set equal to zero. Thus, comparisons of predicted and observed surface waves for explosions at significantly different HOB can provide a definitive test of the adopted source approximation for near-surface bursts.

2.2 AIRBLAST LOADING FROM ATMOSPHERIC EXPLOSIONS

The analytic surface wave simulations conducted to date have dealt exclusively with surface explosions, and the extension to atmospheric explosions with arbitrary HOB requires some modifications in the prediction procedure. In particular, although equation (1) is still valid, a modified expression is required for the airblast loading, p(r,t), and its corresponding Fourier transform, $p(r,\omega)$. For this purpose, we have adopted Brode's recently revised approximation (Speicher and Brode, 1981) which expresses the overpressure for a given yield (W) and HOB as a function of range and time through products of functions involving fairly elaborate polynomial fits to the characteristics of airblasts observed from surface and atmospheric nuclear explosions. The principal features of the overpressure time histories predicted by this model are illustrated schematically in Figure 2. Note that the model predicts only the positive phase of the overpressure beginning at the shock arrival time t_a and having duration D_p. Also, in contrast to the overpressure observed from surface bursts which monotonically decay from a peak

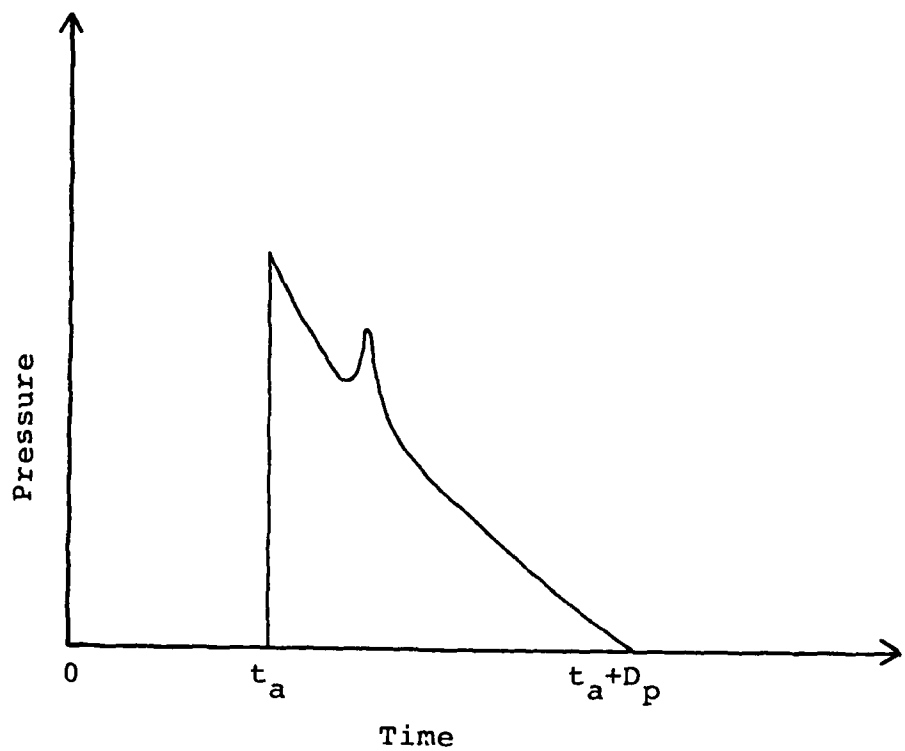

Figure 2. Schematic illustration of overpressure time history predicted by the Speicher and Brode (1981) approximation.

value at the shock arrival time $t = t_a$, the overpressure from HOB explosions can show significant secondary peaks, such as that indicated in Figure 2, as a result of the Mach reflection of the incident shock wave from the free surface. Thus, in general, finer time resolution is required to adequately define the characteristics of the airblast loading induced by HOB explosions.

Some of the prominent characteristics of the airblast loading as a function of HOB at W = 1 kt are illustrated in Figures 3-6. Figure 3 compares the peak incident pressure, $p(t_a)$, as a function of range for HOB of 0, 100 and 500 m. As might be expected, at ranges less than the HOB, the predicted peak pressures for atmospheric explosions are considerably lower than those predicted for a corresponding surface burst. However, the low frequency components of the induced ground motions are relatively insensitive to variations in peak pressure and it is necessary to consider how the other characteristics of the overpressure time histories vary with HOB. Figure 4 compares shock arrival time, t_a, and duration of positive phase, D_p, as a function of range for a surface burst and an atmospheric explosion with HOB = 500 m. Again, for ranges less than the HOB, the D_p values for the two cases differ significantly, indicating changes in the time history of the airblast loading in the vicinity of ground zero. This is illustrated more specifically in Figure 5 which compares the overpressure time histories as a function of HOB at a range of 100 m. It can be seen that although the peak pressure decreases with increasing HOB, as predicted in Figure 3, this effect on the positive phase impulse is largely offset by the increase in D_p with HOB. The corresponding overpressure time histories as a function of HOB at a range of 1000 m are compared in Figure 6. This figure illustrates that at ranges greater than the largest HOB, the airblast loading is relatively insensitive to HOB.

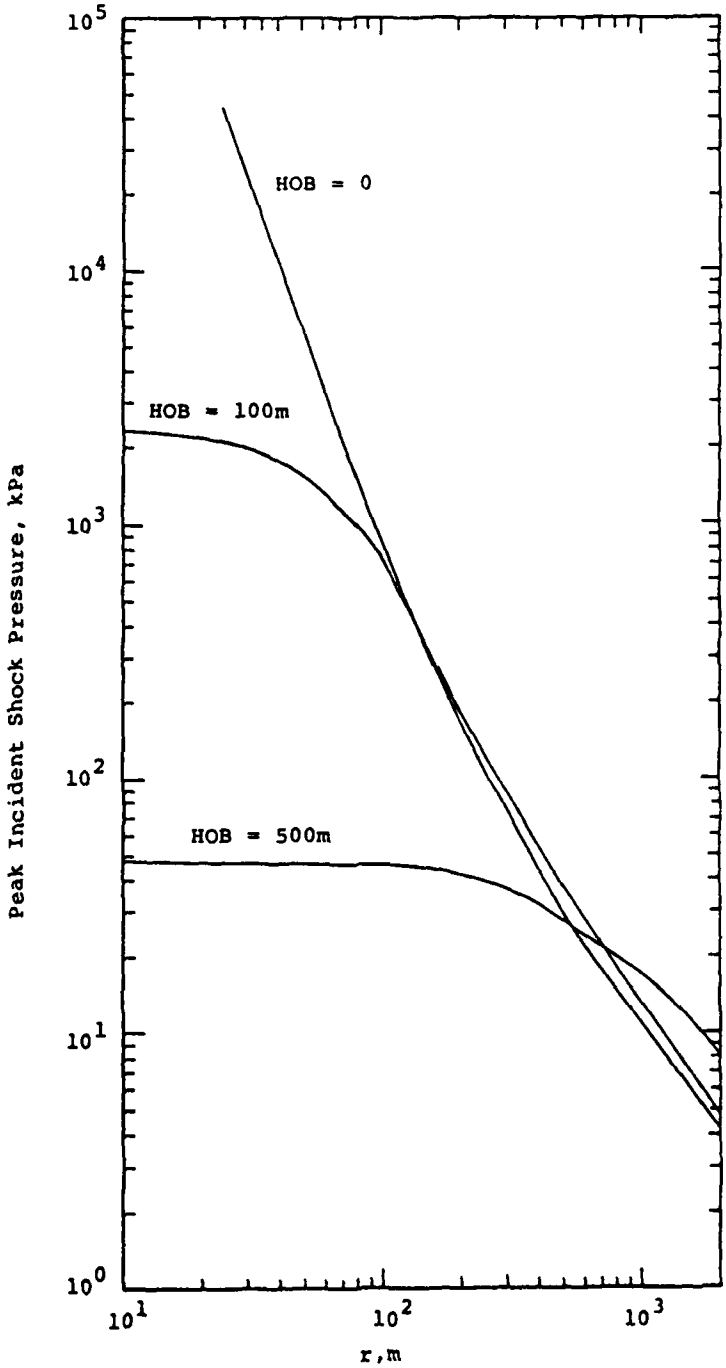

Figure 3. Peak incident pressure as a function of range and HOB, W = 1 kt.

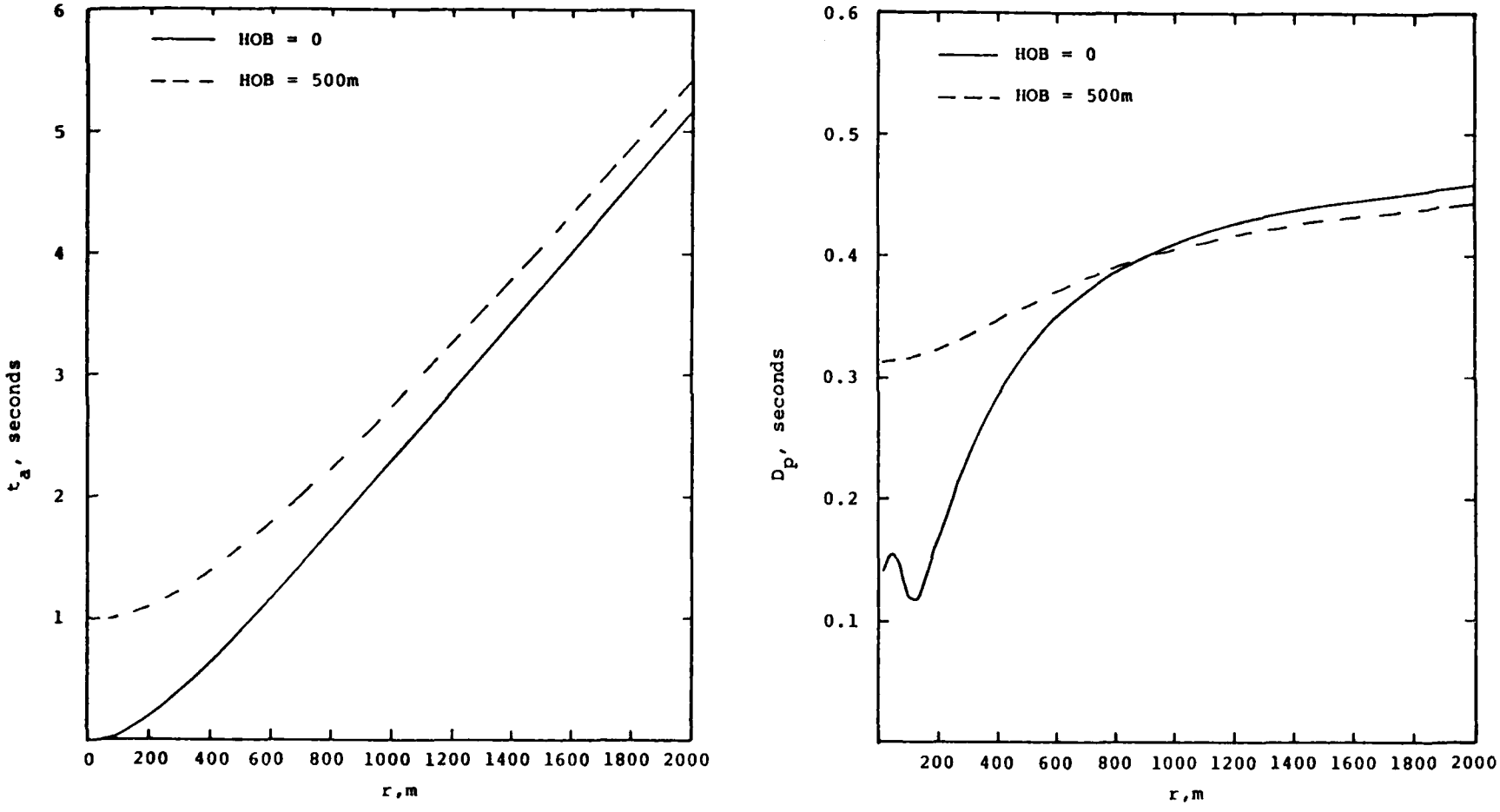

Figure 4. Shock arrival time t_a (left) and positive phase duration D_p (right) as a function of range and HOB, W = 1 kt.

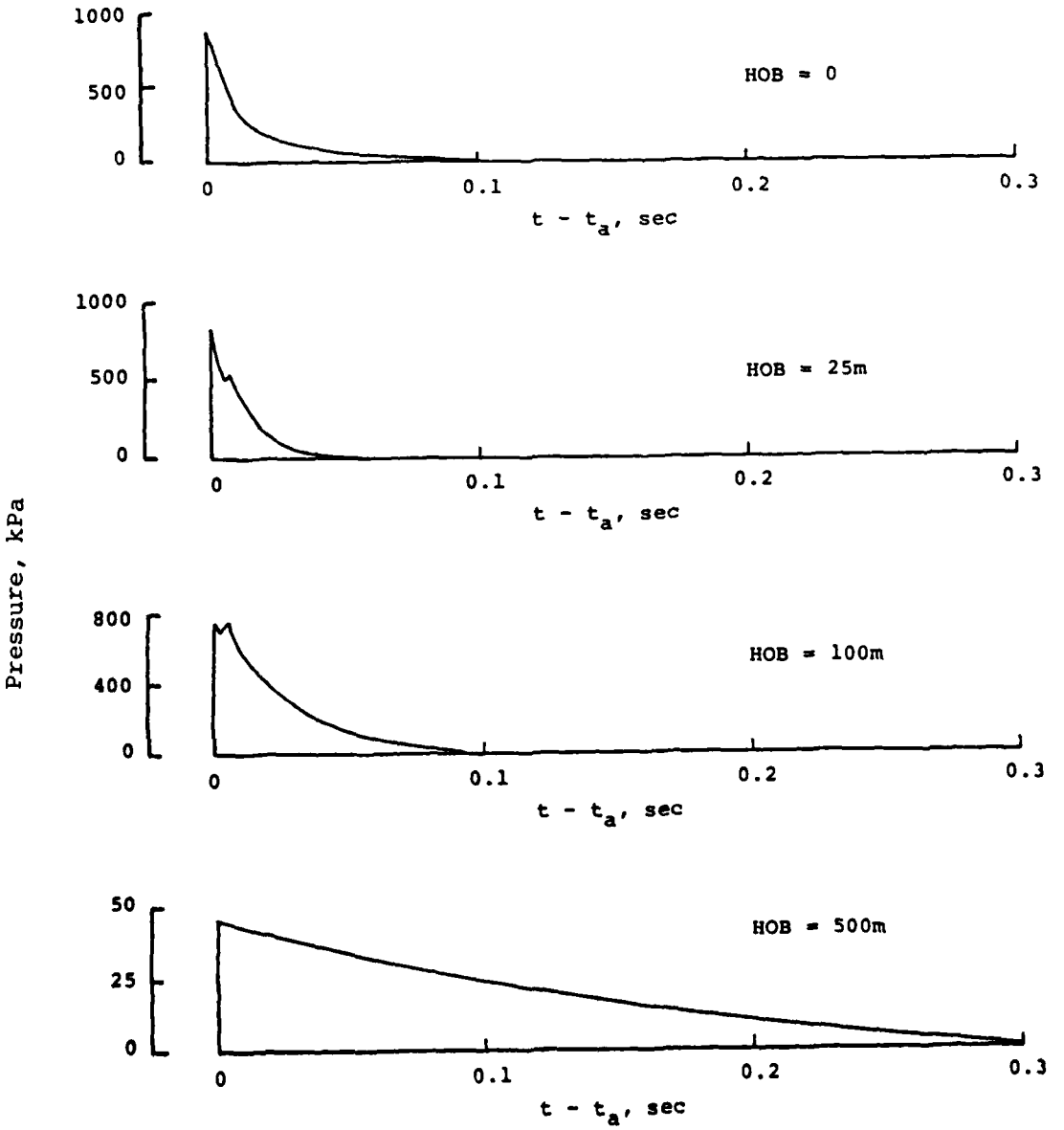

Figure 5. Overpressure time histories as a function of HOB at a range of 100 m, W = 1 kt.

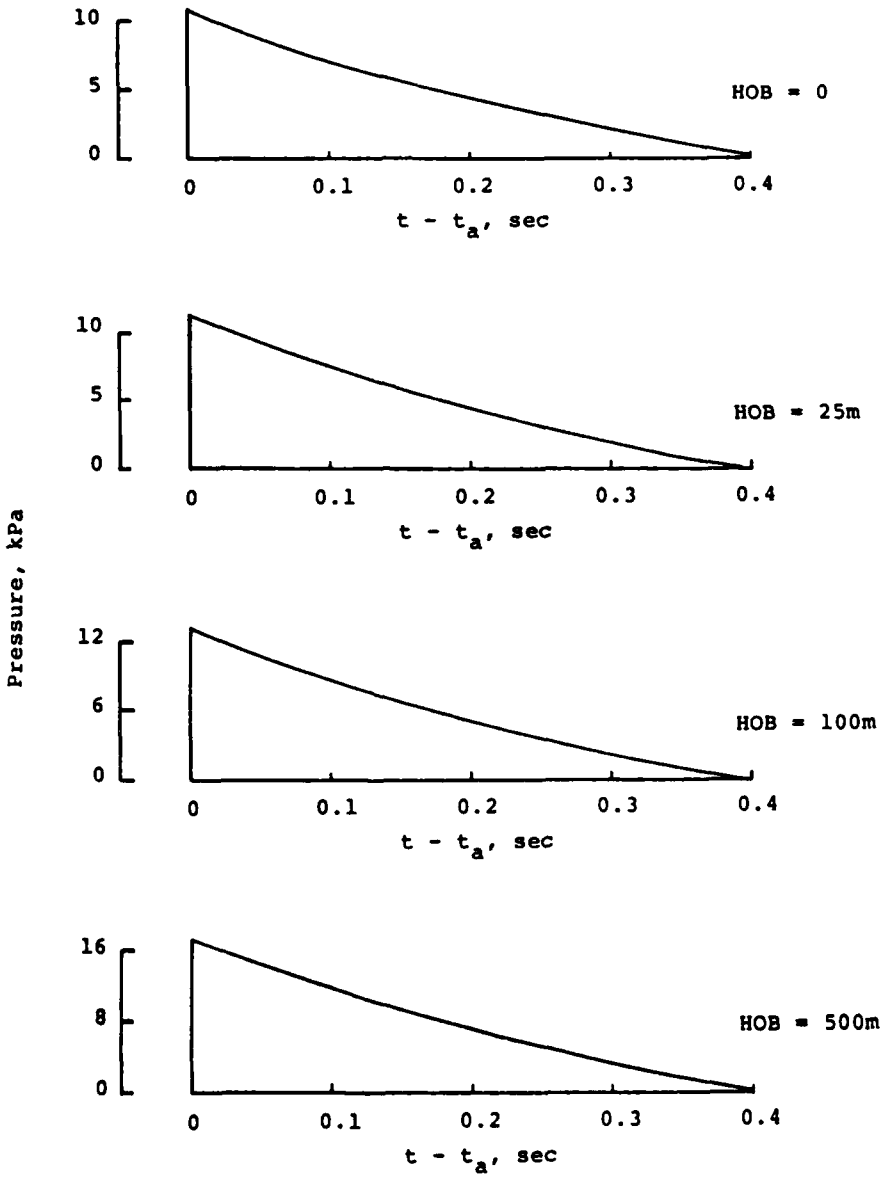

Figure 6. Overpressure time histories as a function of HOB at a range of 1000 m, W = 1 kt.

The results shown in Figures 3-6 indicate that the airblast loading shows a complicated dependence on HOB which can be expected, in general, to have corresponding, frequency-dependent effects on the induced surface waves. However, as has been noted previously (Murphy and Bennett, 1980), some simplifications are possible in the low frequency limit. That is, as $\omega \rightarrow 0$, the amplitude of the airblast-induced Rayleigh waves are directly proportional to the total impulse delivered by the airblast over the loaded area. Figure 7 shows the total impulse as a function of HOB delivered by a 1 kt explosion inside a radius of 2 km from ground zero (*i.e.*, the radius at which the peak overpressure drops to a level of about 1 psi). It can be seen that this total impulse varies by less than a factor of 1.5 for HOB extending from 0 to 500 m. Thus, despite the orders of magnitude variations in peak pressure shown in Figure 3, the total impulse is relatively insensitive to HOB, which suggests that the low frequency components of the induced ground motions will not be very strongly dependent on HOB. This dependence will be explored more explicitly in the following Sections 2.3 and III.

For applications employing equation (1); the Fourier transform of the overpressure, $p(r,\omega)$, is required and it is not feasible to compute this analytically from the $p(r,t)$ given by the complex polynomial approximations of Speicher and Brode (1981). Thus, a numerical Fourier transform procedure must be employed. A problem arises, however, in that the overpressure time histories are often only a fraction of a second in total duration (cf. Figure 5). Thus, the lowest nonzero frequency provided by a numerical Fourier transform routine will be on the order of 10 Hz, while the interest for surface wave simulation purposes is almost always in components of the motion with frequencies less than a few Hertz. Thus, a procedure is required for interpolating the numerical Fourier transform values in the frequency range of interest.

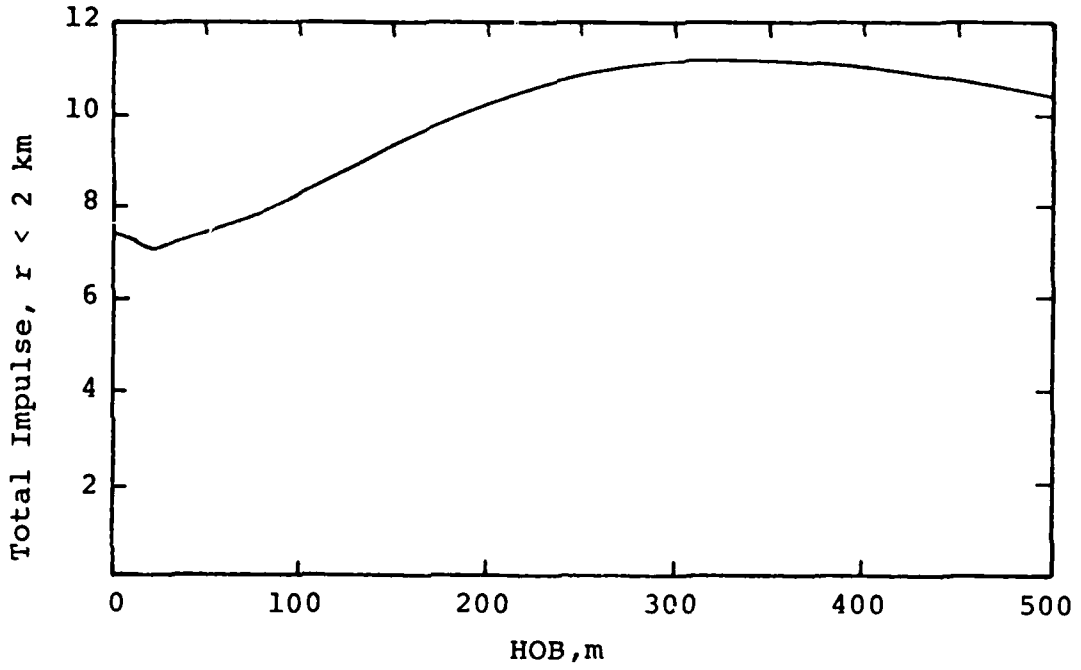

Figure 7. Total impulse delivered to the ground within 2 km of ground zero as a function of HOB, W = 1 kt.

This problem has been extensively studied (*e.g.*, Papoulis, 1962) and the solution for the present application may be summarized as follows. Suppose the overpressure at a given range, $p(\tau)$, is defined such that $p(\tau) = 0$ for $\tau < 0$ and $\tau > 2T$ with $\tau = t - t_a$. Then, it follows that its Fourier transform can be expressed in the form

$$p(\omega) = \int_0^{2T} p(\tau)\, e^{-i\omega\tau}\, d\tau \tag{2}$$

Then, by definition

$$p_n \equiv p\left(\frac{n\pi}{T}\right) = \int_0^{2T} p(\tau)\, e^{-i\,\frac{n\pi}{T}\,\tau}\, d\tau \tag{3}$$

On the other hand, if $p(\tau)$ is expanded in a Fourier series in the interval $0 \le \tau \le 2T$, one obtains

$$p(\tau) = \sum_{n=-\infty}^{\infty} \alpha_n\, e^{in\,\frac{\pi}{T}\,\tau} \tag{4}$$

where

$$\alpha_n = \frac{1}{2T} \int_0^{2T} p(\tau)\, e^{-in\,\frac{\pi}{T}\,\tau}\, d\tau \tag{5}$$

It follows from (3) and (5) that

$$\alpha_n = \frac{p_n}{2T} \tag{6}$$

and a substitution of (6) and (4) into (2) gives

$$p(\omega) = \int_0^{2T} \sum_{n=-\infty}^{\infty} \alpha_n e^{in\frac{\pi}{T}\tau} e^{-i\omega\tau} d\tau$$

$$= \sum_{n=-\infty}^{\infty} \frac{p_n}{2T} \int_0^{2T} e^{-i(\omega - \frac{n\pi}{T})\tau} d\tau \qquad (7)$$

But

$$\int_0^{2T} e^{-i(\omega - \frac{n\pi}{T})\tau} d\tau = T\left[\frac{\sin 2(\omega T - n\pi)}{(\omega T - n\pi)} - i\,\frac{2\sin^2(\omega T - n\pi)}{(\omega T - n\pi)}\right] \qquad (8)$$

and thus we can write

$$p(\omega) = \sum_{n=-\infty}^{\infty} p(\tfrac{n\pi}{T})\ \frac{\sin(\omega T - n\pi)}{(\omega T - n\pi)}\ e^{-i(\omega T - n\pi)} \qquad (9)$$

Finally, using the identity

$$e^{in\pi} \sin(\omega T - n\pi) = \sin \omega T \qquad (10)$$

we obtain

$$p(\omega) = e^{-i\omega T} \sin \omega T \sum_{n=-\infty}^{\infty} \frac{p(\frac{n\pi}{T})}{(\omega T - n\pi)} \qquad (11)$$

Setting $p = p_R + i\,p_I$, the interpolation algorithms for the real and imaginary parts of the Fourier transform of the pressure function take the form

$$p_R(\omega) = \sin \omega T \sum_{n=-\infty}^{\infty} \frac{p_R(\frac{n\pi}{T}) \cos \omega T + p_I(\frac{n\pi}{T}) \sin \omega T}{(\omega T - n\pi)}$$

$$p_I(\omega) = \sin \omega T \sum_{n=-\infty}^{\infty} \frac{p_I(\frac{n\pi}{T}) \cos \omega T - p_R(\frac{n\pi}{T}) \sin \omega T}{(\omega T - n\pi)} \qquad (12)$$

which expresses the Fourier transform of the overpressure at an arbitrary frequency ω in terms of the evenly spaced values obtained from the numerical Fourier transform. In actual applications, the pressure at a given range is nonzero over the time interval extending from t_a to $t_a + D_p$. Thus, we set $T = D_p/2$ in (12) and then the required values of the real and imaginary parts of the pressure ($\tilde{p}_R$, $\tilde{p}_I$), referenced to real time t, are given by

$$\tilde{p}_R(\omega) = p_R(\omega) \cos \omega t_a + p_I(\omega) \sin \omega t_a$$

$$\tilde{p}_I(\omega) = p_I(\omega) \cos \omega t_a - p_R(\omega) \sin \omega t_a \qquad (13)$$

2.3 SIMULATED RAYLEIGH WAVES FROM EXPLOSIONS WITH DIFFERENT HOB

In order to illustrate the simulation of Rayleigh waves as a function of HOB, we will consider a preliminary application to a subsurface geologic model characteristic of the Yucca Flat testing area on the Nevada Test Site. Estimates of the relevant subsurface geophysical parameters (compressional and shear wave velocities α and β and density ρ) for this site are illustrated graphically in Figure 8 (Hays and Murphy, 1971). It can be seen that the area is characterized by thick layers of alluvium and tuff overlying the Paleozoic basement rocks. The fundamental mode Rayleigh wave dispersion curves computed using this model are shown in Figure 9, where it can be seen that there is a well-developed group velocity minimum in the 0.5 to 1.0 Hz frequency band. As has been noted previously (Murphy and Bennett, 1980), this frequency of minimum group velocity coincides with a corner frequency in the Rayleigh wave site response function and is given approximately by $\bar{\beta}/2H$ where H denotes the depth to the basement and $\bar{\beta}$ denotes the interval-averaged shear wave velocity to that depth. This is illustrated in Figure 10 which

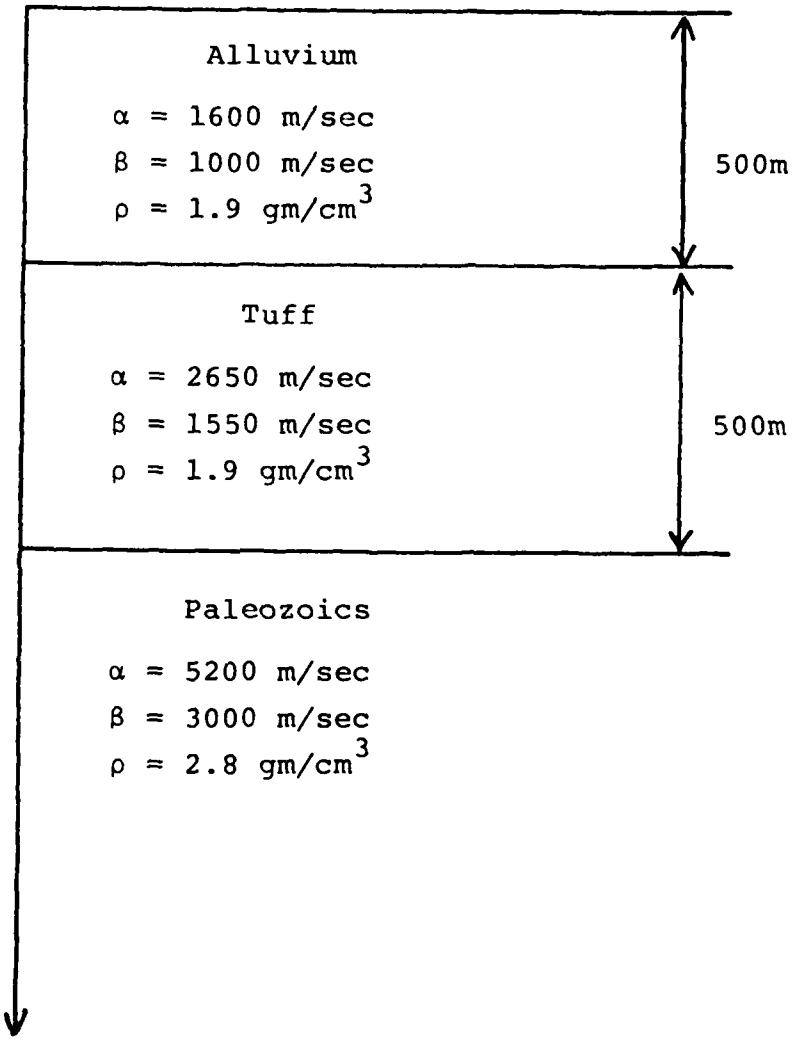

Figure 8. Subsurface geologic model for Yucca Flat simulations.

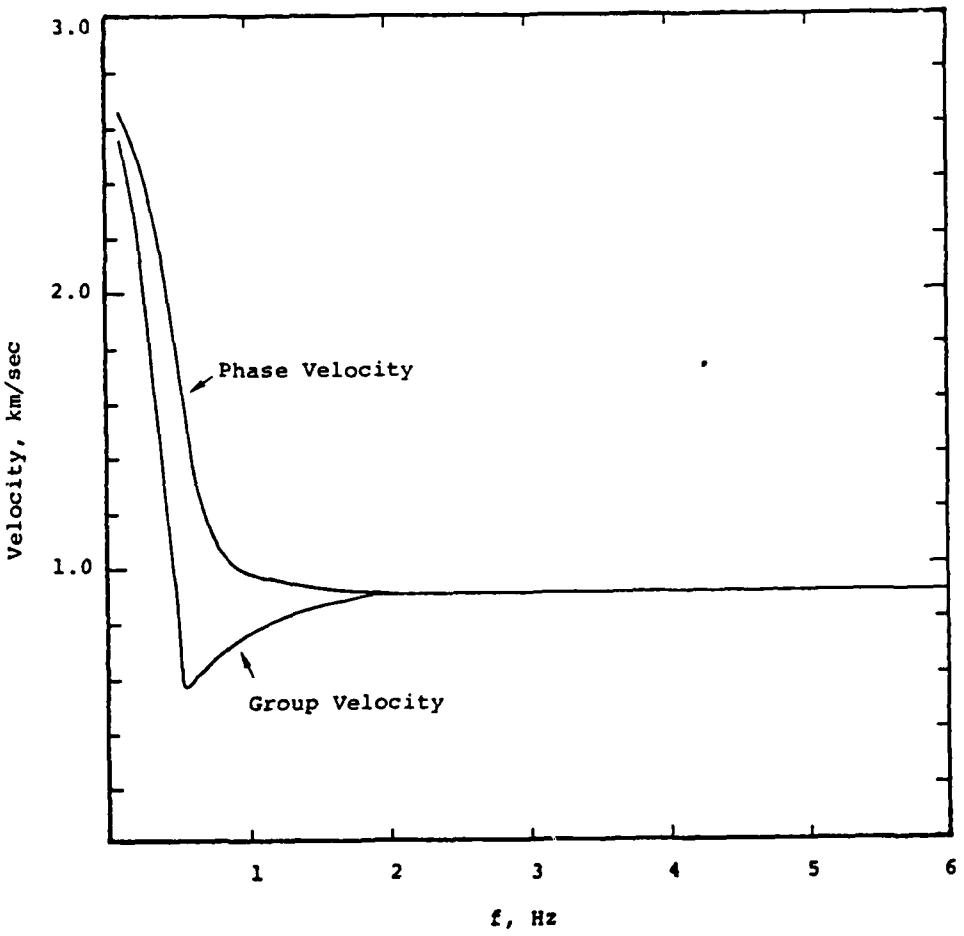

Figure 9. Fundamental mode Rayleigh wave dispersion curves for Yucca Flat model.

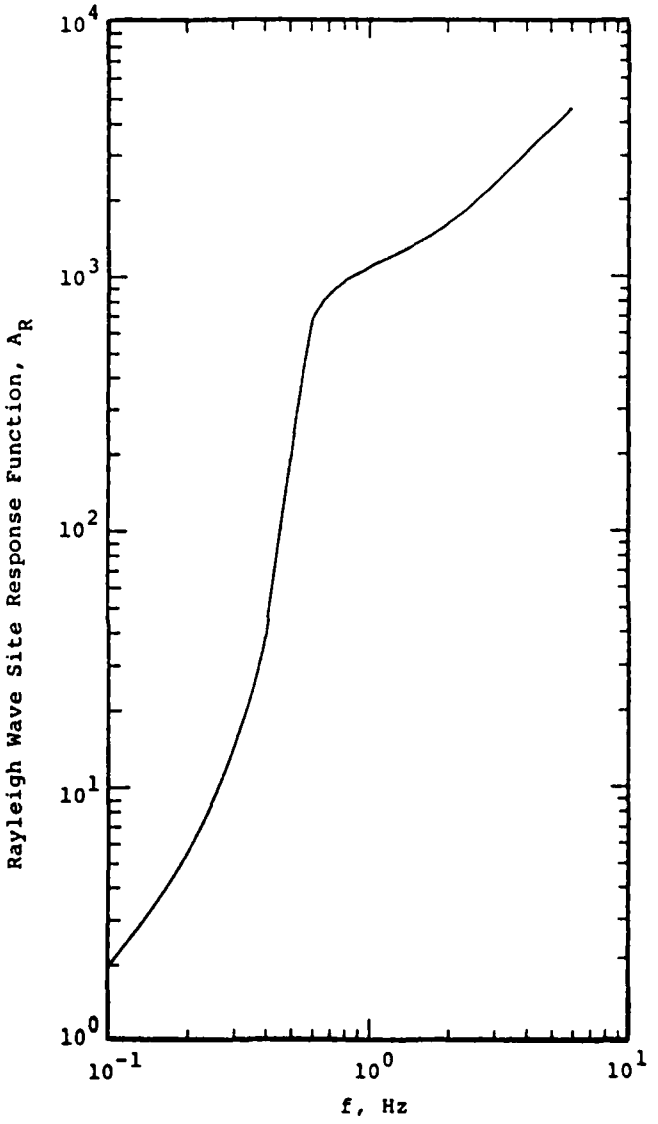

Figure 10. Rayleigh wave site response function for Yucca Flat model.

shows the corresponding Rayleigh wave site response function with a pronounced corner frequency at about 0.7 Hz. For explosions of sufficiently large yield, this corner frequency will define the predominant frequency of the explosion-induced Rayleigh waves (Murphy and Bennett, 1980).

The fundamental mode Rayleigh waves induced in this geologic model by 1 kt explosions with HOB ranging from 0 to 500 m have been computed using equation (1) together with the airblast approximation of Speicher and Brode (1981). The resulting Rayleigh wave displacement spectra at a range of 2500 m from 1 kt explosions at HOB of 100 and 500 m are compared in Figure 11. It can be seen that the high frequency content of the signal decreases significantly with increasing HOB over this range. This presumably reflects the relatively low frequency character of the incident overpressure near ground zero for the higher altitude explosion (cf. Figure 3). However, these spectral differences are most notable in a frequency band within which the spectral amplitudes are an order of magnitude down from the peak level and, thus, contribute little of the time domain signal. In the band between 0.6 and 1.0 Hz, in which the spectral maxima occur, the differences between the two spectra are much less pronounced. Moreover, it has been found that for HOB in the range 0 to 100 m, the Rayleigh wave displacement spectra are essentially identical to that obtained for an HOB of 100 m. Thus, the spectral results suggest that the airblast-induced Rayleigh waves at this site should be relatively insensitive to HOB. This inference is confirmed by Figures 12-14 which show the dependence of the induced Rayleigh waves on HOB at ranges of 500, 1000 and 2500 m, respectively. Comparing Figures 12-14 for a particular value of HOB it can be seen that, as expected, the dominant frequency of the Rayleigh waves at all three ranges fall in the 0.7 to 1.0 Hz band and the predominant effect of increasing range on the signal is the gradual

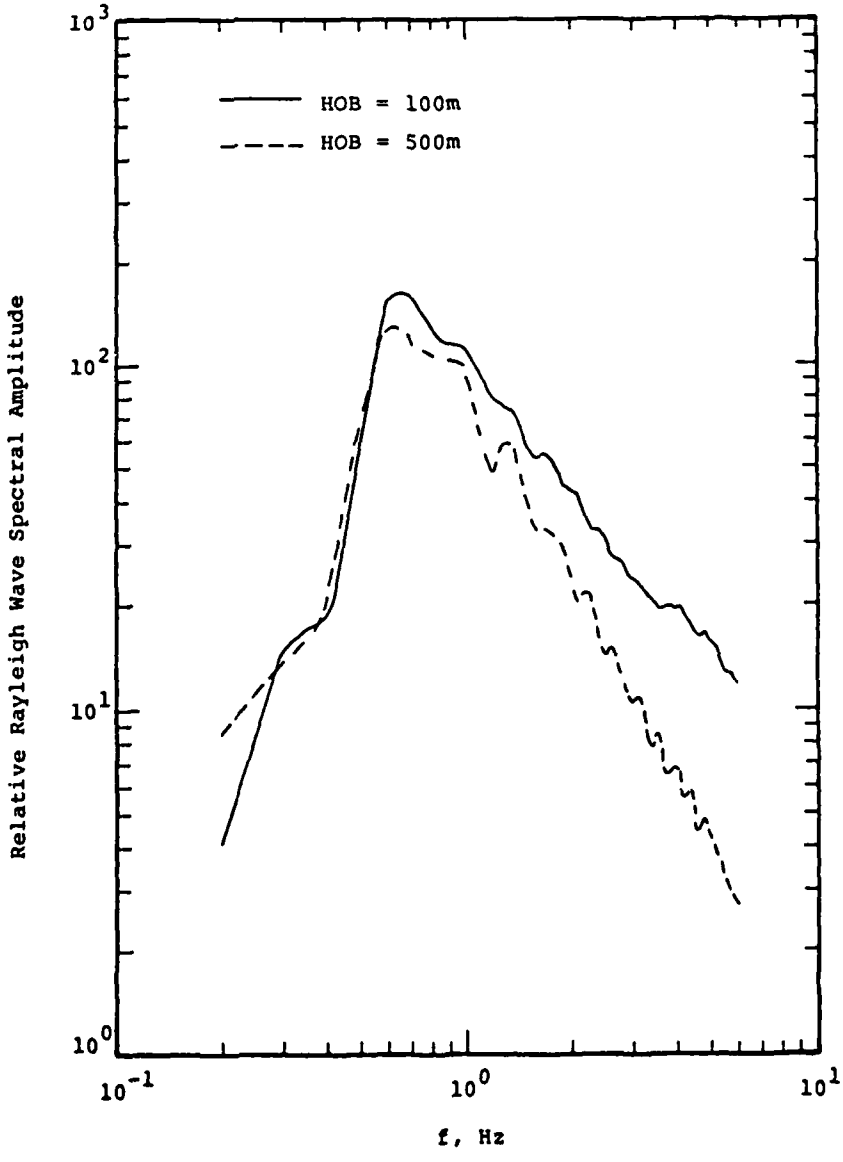

Figure 11. Comparison of Rayleigh wave displacement spectra as a function of HOB at a range of 2500 m, Yucca Flat, W = 1 kt.

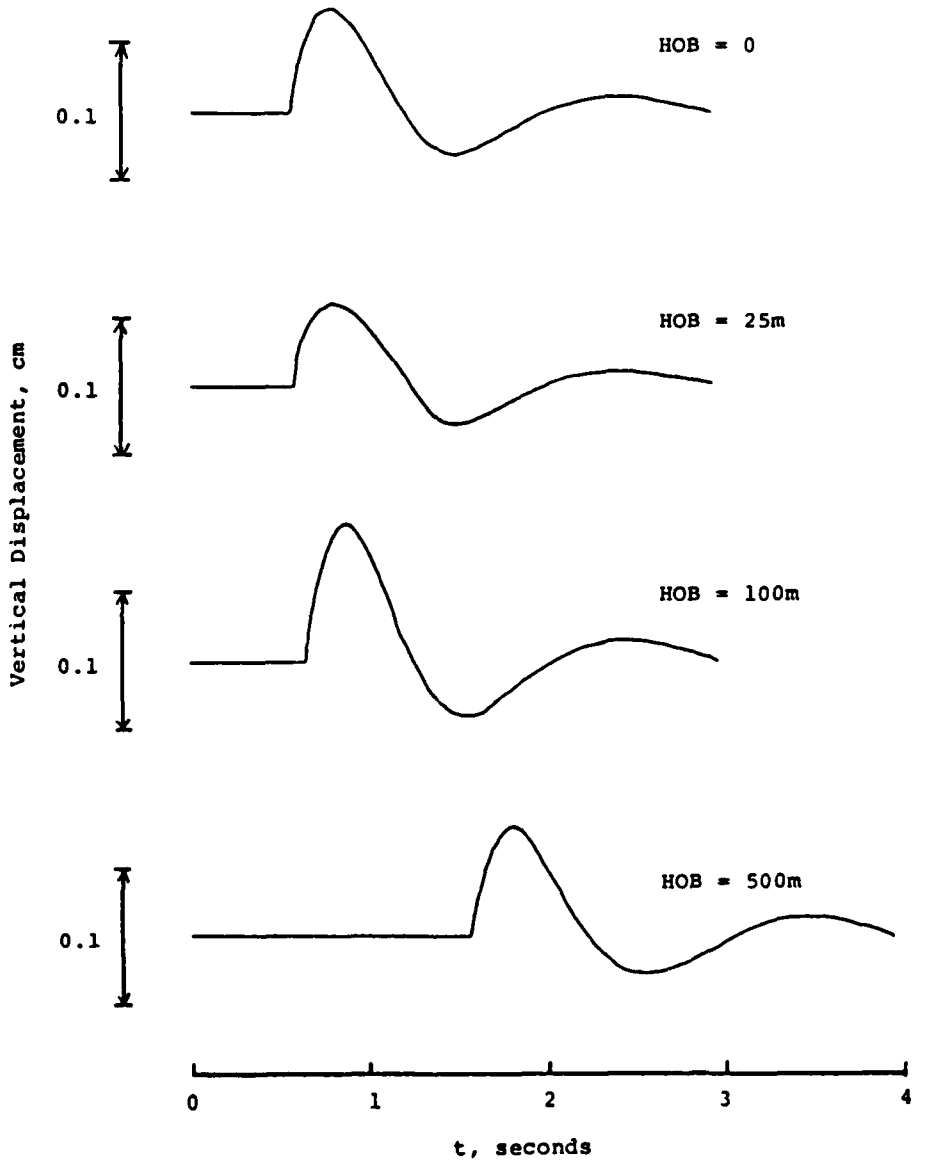

Figure 12. Vertical component Rayleigh wave displacements as a function of HOB at a range of 500 m, Yucca Flat, W = 1 kt.

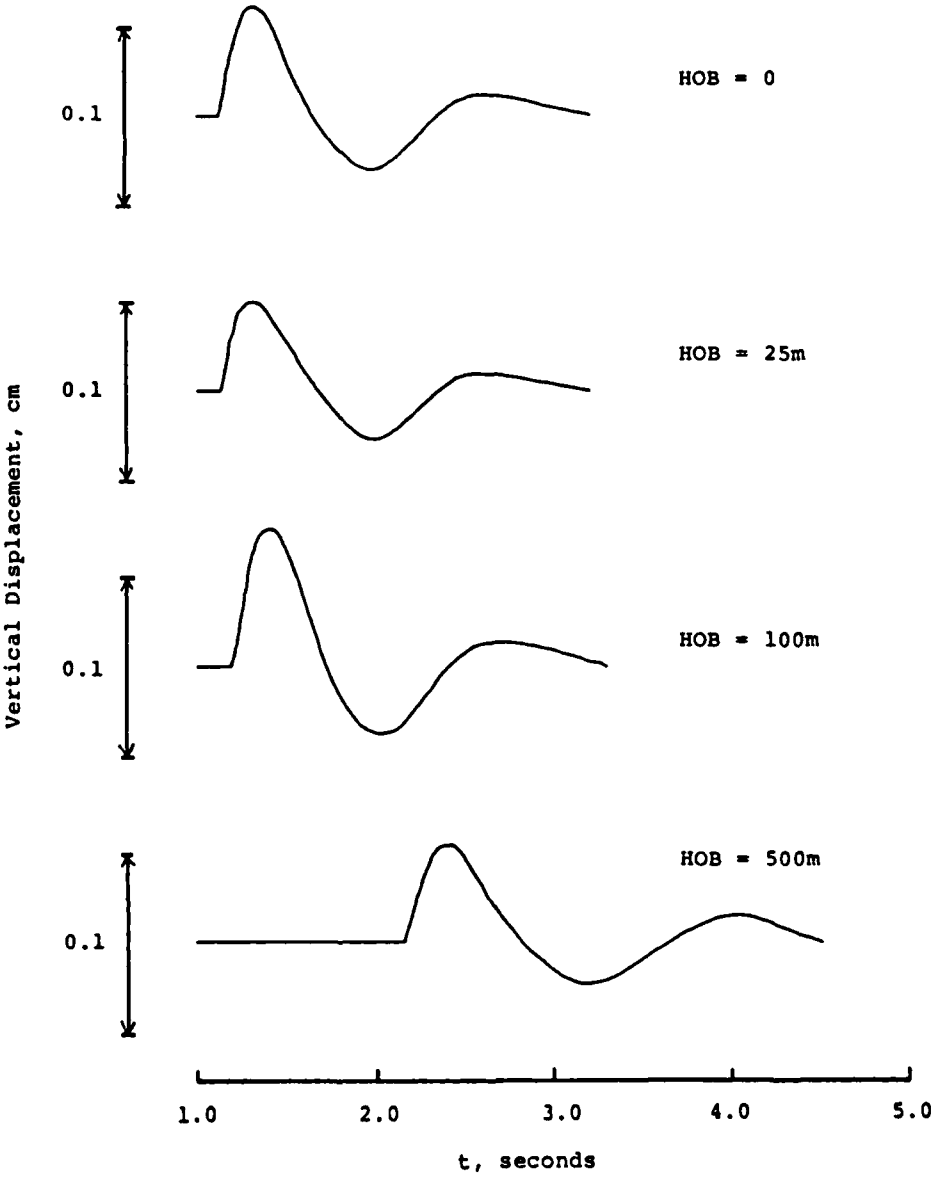

Figure 13. Vertical Component Rayleigh wave displacements as a function of HOB at a range of 1000 m, Yucca Flat, W = 1 kt.

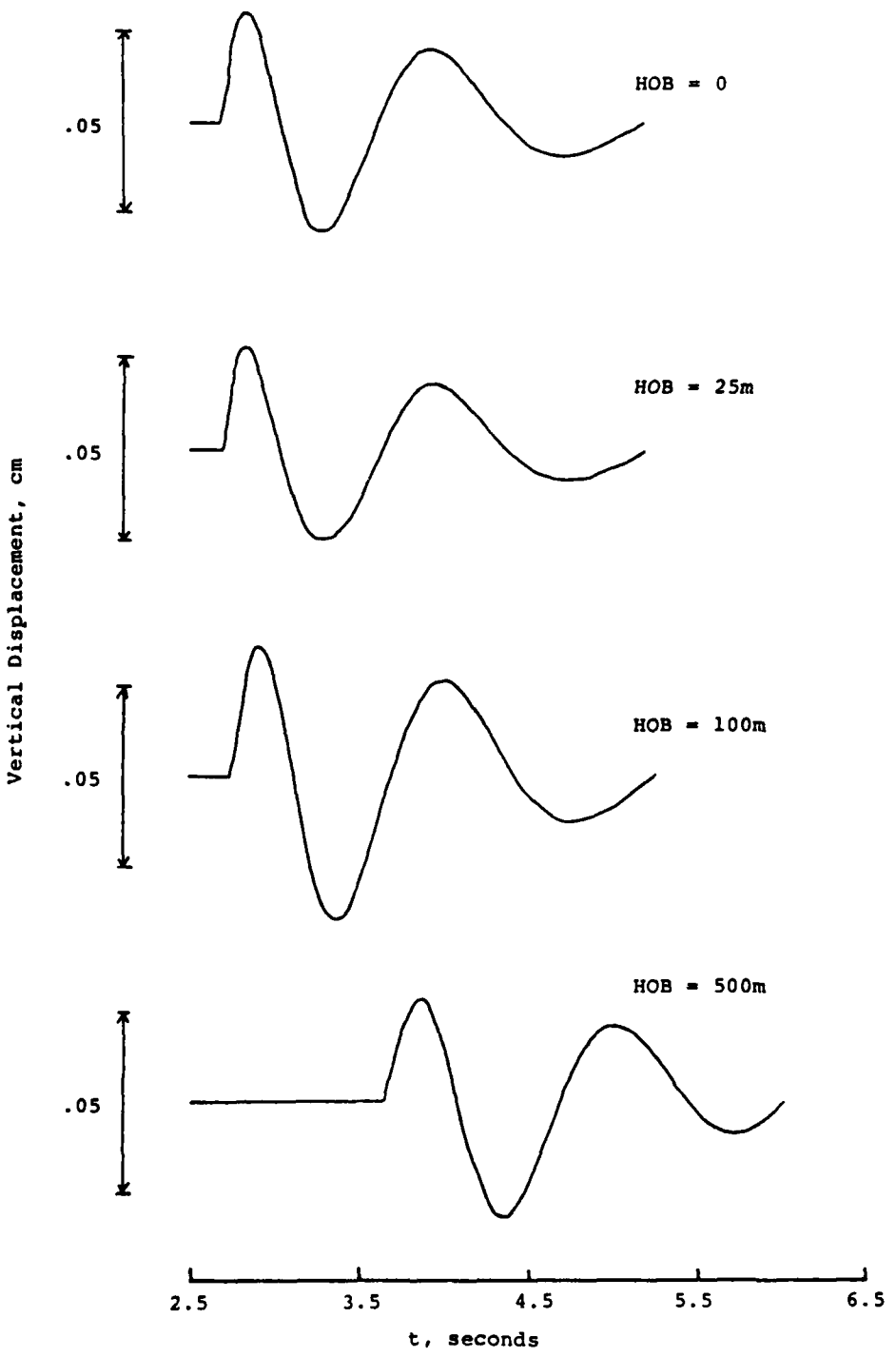

Figure 14. Vertical component Rayleigh wave displacements as a function of HOB at a range of 2500 m, Yucca Flat, W = 1 kt.

dispersion of energy over time due to the frequency dependent propagation velocities of the various components of the signal. Furthermore, it can be seen that at a fixed range, the simulated Rayleigh waves show little variation with HOB over the range from 0 to 500 m. Specifically, the frequency content remains essentially constant and the amplitude level varies by less than a factor of two. Thus, as was inferred from the integrated impulse curve shown in Figure 7, the low frequency airblast-induced Rayleigh waves are relatively insensitive to HOB, at least for this combination of site geology and yield.

III. APPLICATION TO THE PRE-DIRECT COURSE EXPERIMENT

The Pre-Direct Course high explosive (HE) experiment is scheduled to be detonated at the White Sands Test Site in the fall of 1982, near the location of the previous Mill Race experiment. As currently planned, it will consist of 24 tons of HE (ANFO) detonated at an HOB of 16.7 m. Preliminary determinations of subsurface physical properties at the site have been made on the basis of a refraction survey (Personal Communication, Bob Reinke, AFWL, 1982) and are shown schematically in Figure 15 together with the corresponding predicted fundamental mode Rayleigh wave dispersion curves. It should be noted that the shear wave velocities, which control the Rayleigh wave characteristics, have not been measured at this site and, consequently, have been estimated on the basis of results obtained from other sites in this general area. It can be seen that the refraction survey indicates the presence of a thick (75m) layer of dry alluvium overlying saturated alluvium which apparently extends to a depth of more than 150 m (*i.e.*, the approximate limit of resolution of the 500 m long refraction line). Note that because of the small inferred variation of shear wave velocity (β) with depth, very strong dispersion of the surface wave energy is not expected at this site. However, the model does predict a distinct group velocity minimum at a frequency of about 2.5 Hz (*i.e.*, $\beta_1/2H$). As expected, this corresponds to a pronounced corner frequency on the corresponding Rayleigh wave site response function, $A_R(\omega)$, shown in Figure 16. Thus, for this site model, the predominant energy in the surface wave components of the ground motion is expected to be confined to frequencies above 2.5 Hz.

The low frequency ground motions to be expected from this test have been estimated using an airblast loading function computed from the Speicher and Brode (1981) analytic

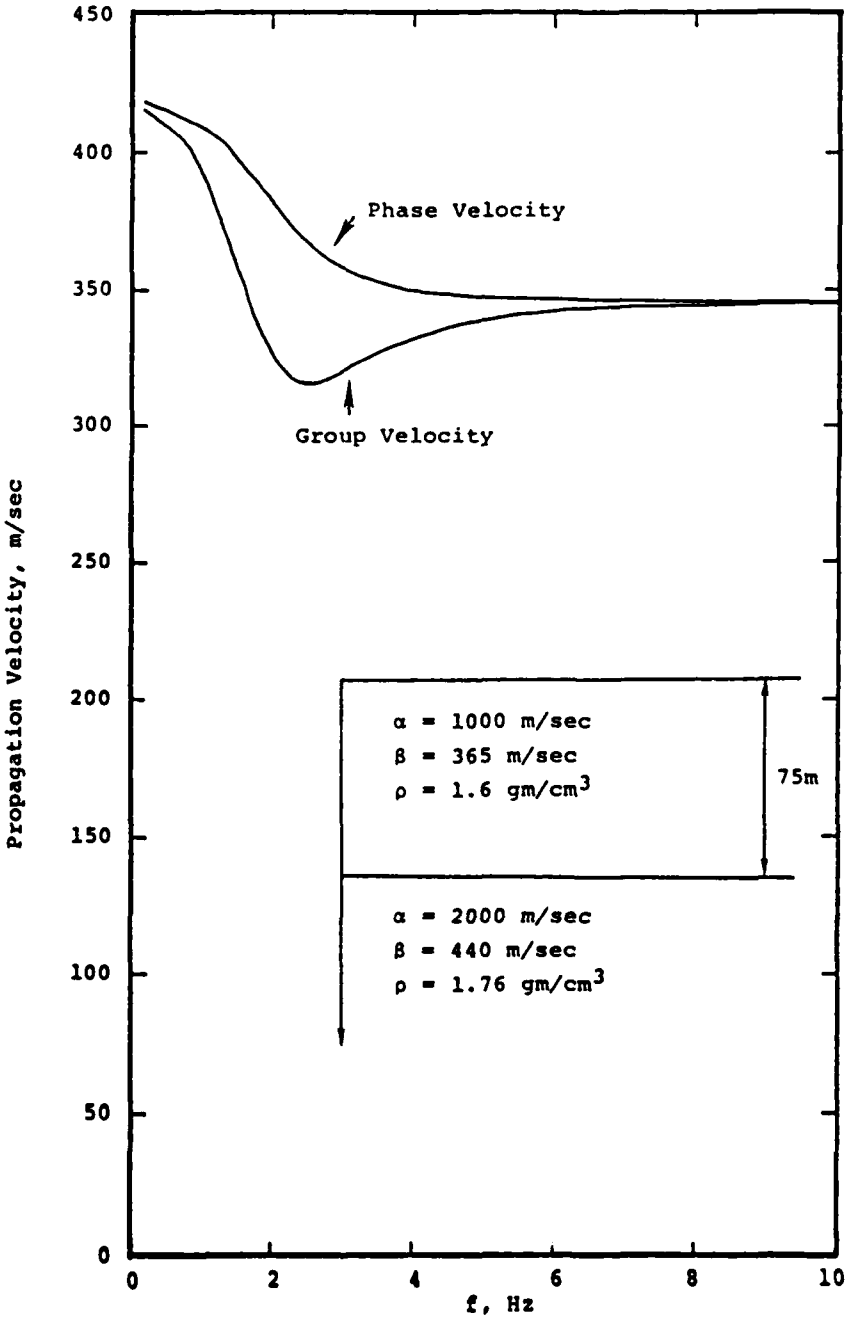

Figure 15. Subsurface geologic model and associated fundamental mode Rayleigh wave dispersion curves, Pre-Direct Course.

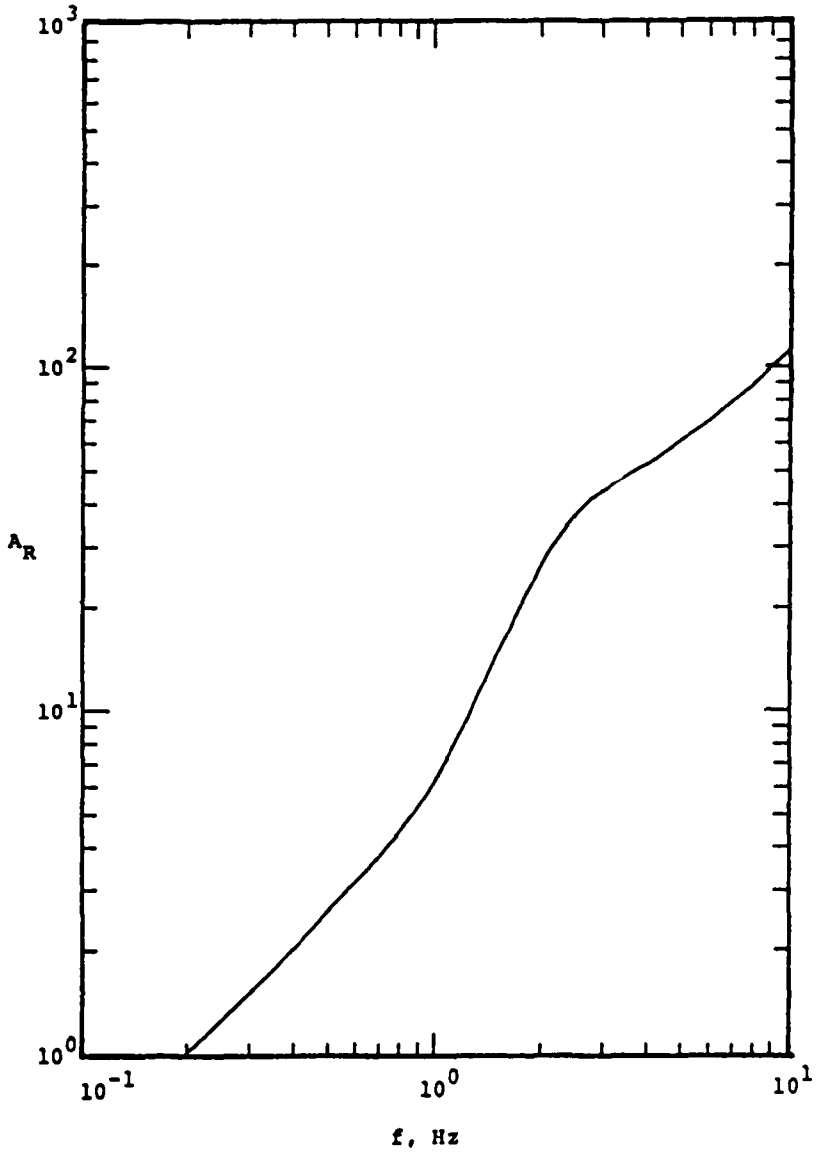

Figure 16. Pre-Direct Course Rayleigh wave site response function (A_R).

approximation for nuclear explosions with an effective yield of 48 tons. Available evidence suggests that a nuclear explosion of this yield will produce an airblast loading essentially equivalent to that expected from the detonation of 24 tons of ANFO at that same height (Personal Communication, George Ullrich, DNA, 1982). Figure 17 shows a comparison of the predicted peak overpressures as a function of range obtained for Pre-Direct Course and a surface burst of the same yield. The surface burst prediction is truncated at a range of 6 m, consistent with the estimated exclusion radius (*i.e.*, r_0) for that yield. It can be seen that the predicted peak pressures are quite different at ranges of less than 15 m and essentially identical at larger ranges.

The airblast induced Rayleigh waves to be expected from Pre-Direct Course, as well as from an expected subsequent companion surface burst experiment of the same yield, have been estimated using the analytical models and numerical procedures described in Section II. Figure 18 shows the predicted vertical component Rayleigh wave displacements for Pre-Direct Course over the horizontal distance range extending from ground zero to 200 m. It can be seen that the predicted waveforms are quite simple and pulse-like, reflecting the simplicity of the adopted subsurface geological model (*i.e.*, the shear wave velocity distribution shown in Figure 15 is nearly independent of depth). The most notable feature of these waveforms is the evidence of multiple arrivals at ranges greater than 100 m. It was initially conjectured that this multiple arrival phenomenon might be associated with the secondary Mach reflection arrival in the airblast loading predicted for the HOB explosion. However, it was subsequently noted that the delay time between the two airblast arrivals is much too short to be associated with the observed delay between the multiple Rayleigh wave arrivals. In fact, the results of numerical modeling experiments suggest this

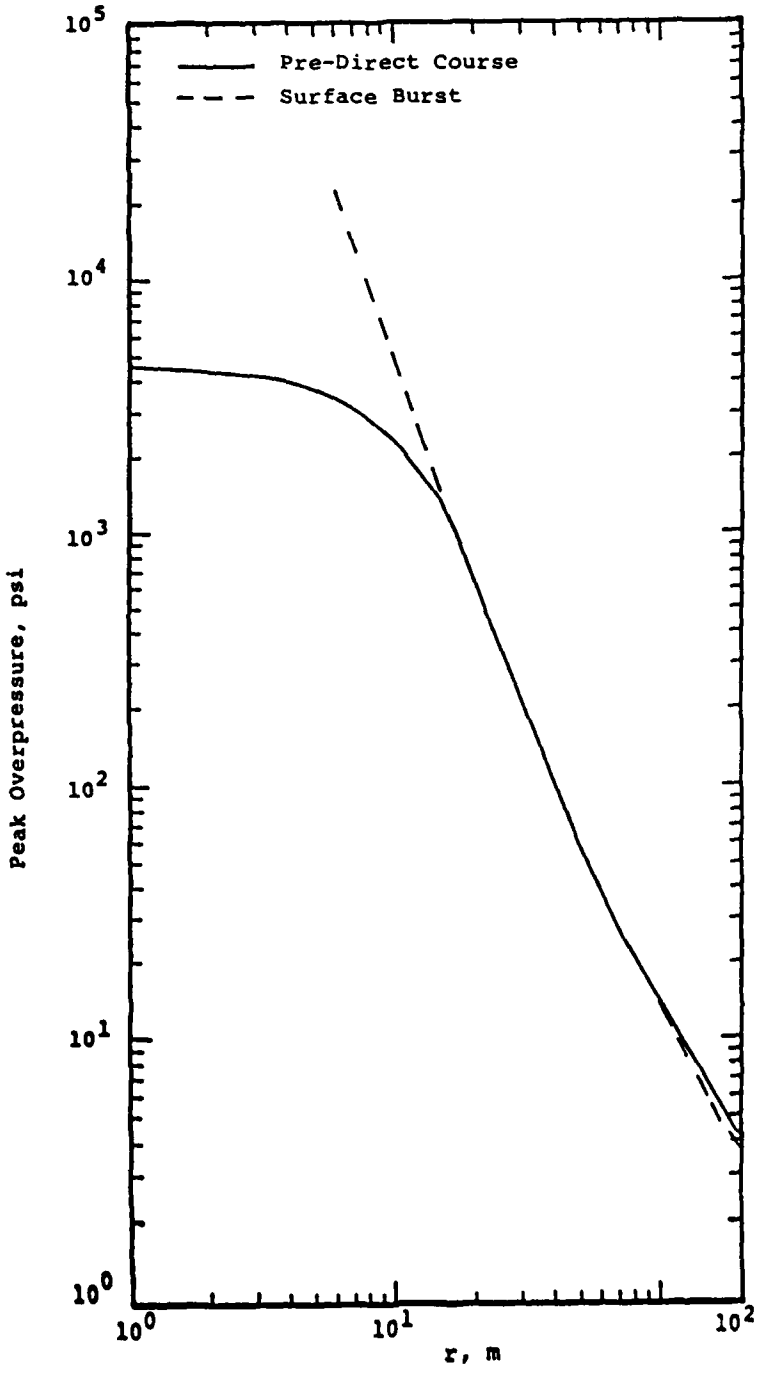

Figure 17. Comparison of peak overpressures as a function of range for Pre-Direct Course and a surface burst test of the same yield.

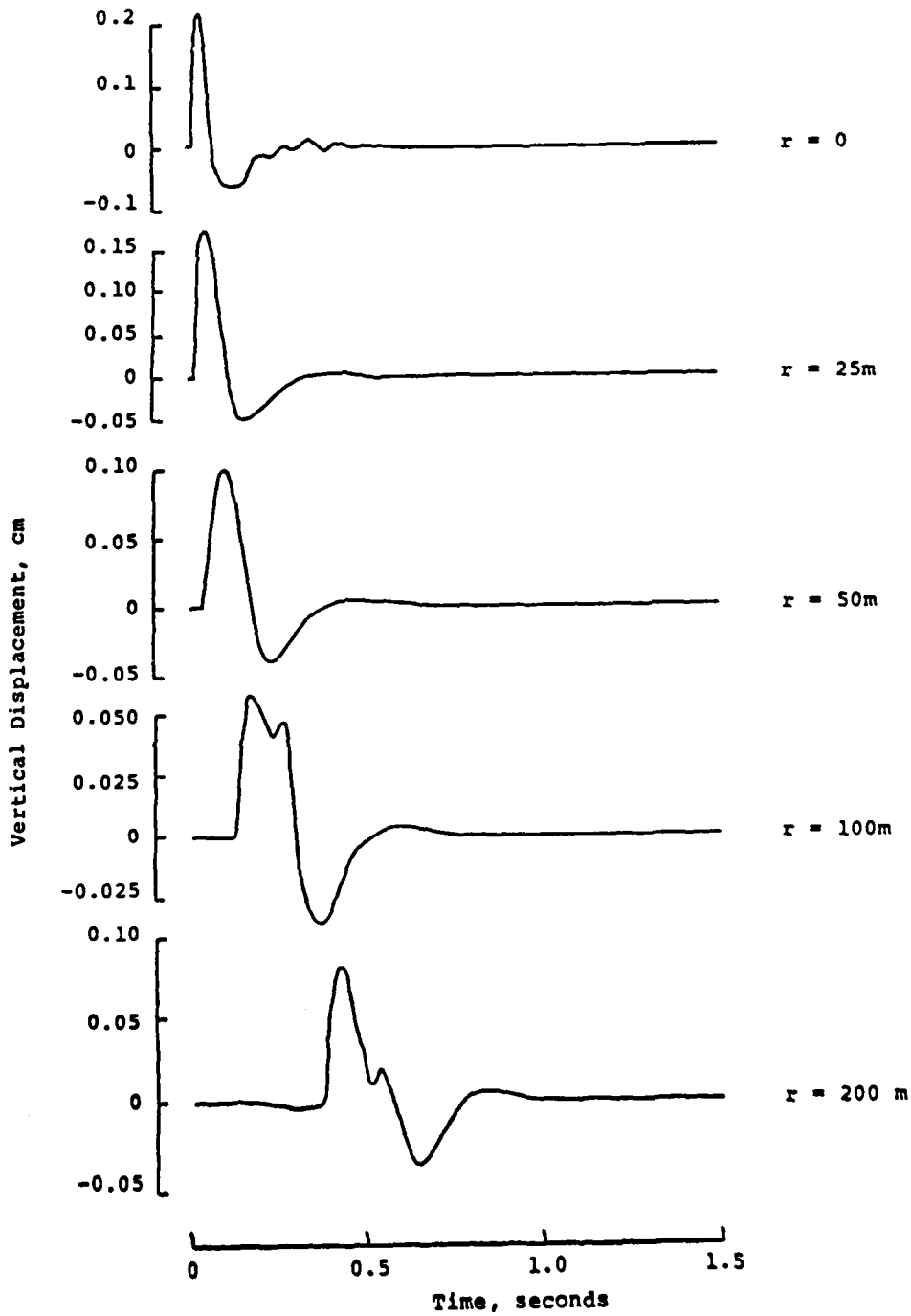

Figure 18. Predicted vertical component Rayleigh wave displacement as a function of range, Pre-Direct Course.

characteristic of the predicted Rayleigh waves is related to the characteristics of the site. That is, the Rayleigh wave coupling for an explosion of this yield for this site model is partitioned into two distinct phases: an initial phase dominated by the loading within about 20 m of ground zero and a secondary phase dominated by the loading in the range from about 50 to 100 m. This is presumably a function of the relationship between the local airblast velocity and the Rayleigh phase velocity distribution characteristic of the site. Thus, the predicted effect is probably strongly dependent on the subsurface shear wave velocity distribution, which is not very well constrained by currently available data.

As in the case of the Yucca Flat nuclear simulations described in Section 2.3, it has been found that the predicted Rayleigh displacements for an equivalent surface burst test are quite similar to those obtained for Pre-Direct Course. This is illustrated in Figure 19 which shows comparisons of the predicted Rayleigh waves for the two explosions at ranges of 25 and 200 m. It can be seen that the predicted peak displacements and waveforms agree to within the expected measurement uncertainty and indicate no pronounced effect of HOB over this range.

Thus, the theoretical simulations of the Rayleigh waves to be expected from the Pre-Direct Course HOB experiment and a surface burst of the same yield suggest that there should be negligible differences in the low frequency ground motions observed from these two tests. It follows that ground motion data recorded from such a pair of experiments conducted at this site would provide an excellent test of the validity of the approximations currently being used to estimate this component of the explosively-generated ground motions.

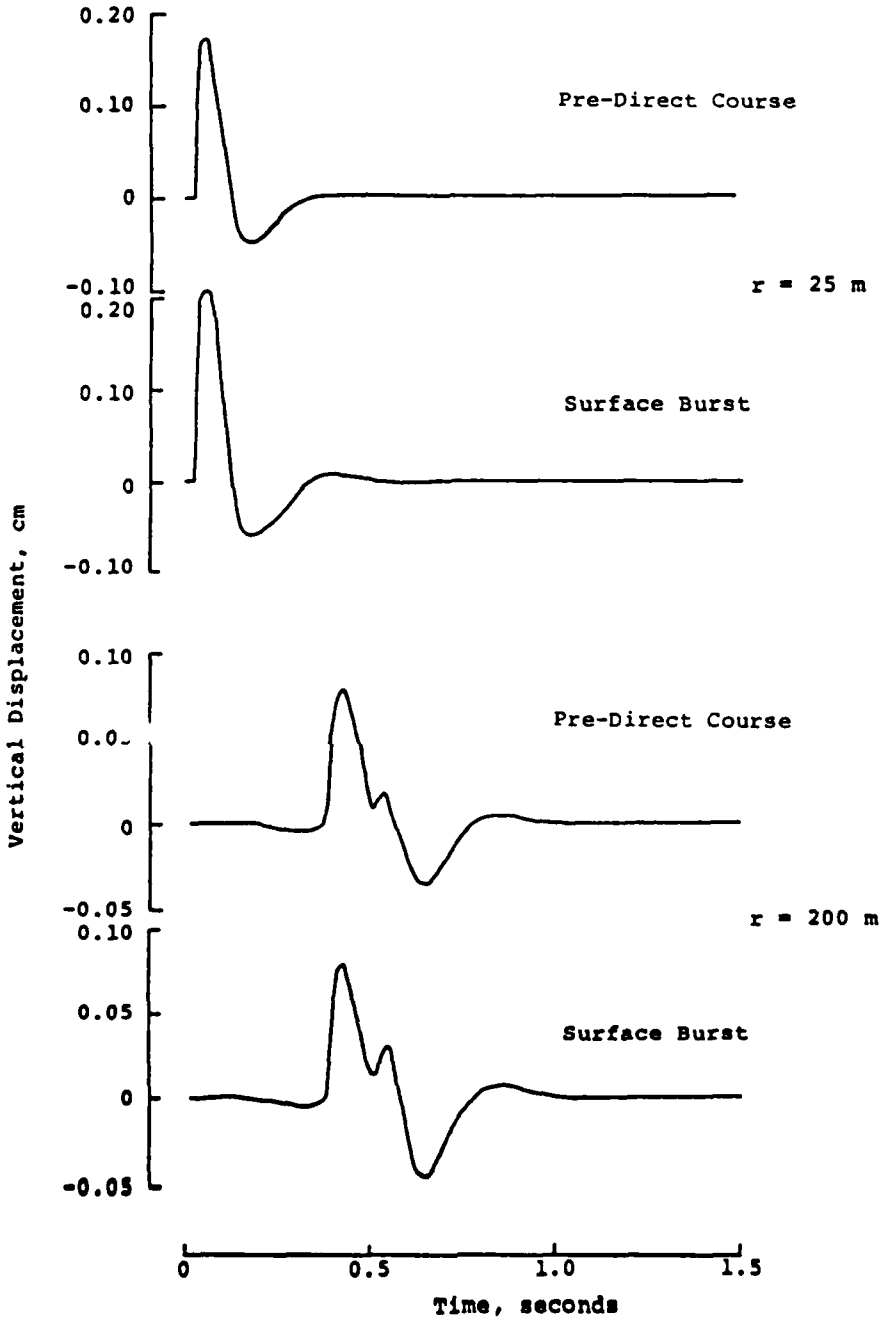

Figure 19. Comparison of predicted vertical component Rayleigh wave displacements for Pre-Direct Course and a surface burst test of the same yield.

IV. SUMMARY AND CONCLUSIONS

4.1 SUMMARY

The investigation summarized in this report has centered on an analysis of the effects of variations of HOB on the low frequency ground motions induced by near-surface and atmospheric explosions. In particular, the present effort has encompassed an extension of the existing analytical model for surface explosions to include consideration of a general airblast loading function valid for arbitrary HOB.

The mathematical model derived to estimate the low frequency ground motions produced by HOB explosions was described in Section II where it was applied to the parametric investigation of the effects of HOB on a prototype 1 kt nuclear explosion detonated over a site model approximating the subsurface geology at Yucca Flat on the Nevada Test Site. The generalized airblast loading function proposed by Speicher and Brode (1981) was adopted for modeling purposes and a detailed numerical procedure was derived for incorporating this loading function into the analytical Rayleigh wave prediction model. The results of the parametric investigation of the Yucca Flat site model were analyzed in both the frequency and time domains and it was found that, despite the fact that the characteristics of the airblast loading changes significantly with increasing HOB, the corresponding induced surface waves are relatively insensitive to HOB. That is, it was found that the low frequency coupling of interest with regard to surface wave generation is not very sensitive to HOB, at least for this combination of site geology and yield.

The estimation of the characteristics of the low frequency ground motions to be expected from the Pre-Direct Course HOB experiment was addressed in Section III where predictions of near-field ground motions were presented for this event as well as for a hypothetical surface burst test

of the same yield at that site. It was shown that the surface waves predicted on the basis of the currently available subsurface model of the site are quite simple and pulse-like and show little dependence on HOB over the range considered.

4.2 CONCLUSIONS

The analyses summarized above support the following conclusions regarding the effects of HOB on the low frequency ground motions induced by near-surface and atmospheric explosions.

1. Despite the fact that the airblast loading from explosions varies significantly with HOB, the total integrated impulse delivered to the ground by the propagating airblast, which defines the low frequency limit of the surface wave coupling coefficient, is relatively insensitive to HOB for scaled HOB in the range from 0 to 500 $m/kt^{1/3}$.

2. Simulated Rayleigh waves from 1 kt explosions over a site model approximating the subsurface geology at Yucca Flat on the Nevada Test Site were found to be essentially independent of HOB for HOB ranging from 0 to 500 m. This is consistent with Cooper's (1972) observation that the peak displacement data recorded from nuclear airblasts at NTS are not strongly dependent on HOB.

3. Predicted surface wave ground motions for the proposed Pre-Direct Course HE experiments and a hypothetical surface burst test of the same yield also show little dependence on HOB. For this reason, it is concluded that such a pair of experiments would provide an excellent

opportunity to test the validity of approximations currently being used to estimate the low frequency components of the ground motions produced by near-surface and atmospheric explosions.

REFERENCES

Auld, H. E. and J. R. Murphy (1979), "Surface Wave Calculations," Paper presented at the Defense Nuclear Agency Strategic Structures Division Biennial Review Conference, Menlo Park, California.

Brode, H. L. (1968), "Review of Nuclear Weapons Effects," Annual Review of Nuclear Science, 18, pp. 153-202.

Cooper, H. F. (1972), "On Strong-Motion Seismic Ground Motions From Nuclear Air Burst Explosions," RDA-TR-063-DNA, RDA Associates, Santa Monica, California.

Hays, W. W. and J. R. Murphy (1971), "The Effect of Yucca Fault on Seismic Wave Propagation," Bull. Seism. Soc. Am., 61, p. 697.

Murphy, J. R. (1978), "An Analysis of the Characteristics of Rayleigh Waves Produced by Surface Explosions," Final Technical Report to the Defense Nuclear Agency, DNA 4826F.

Murphy, J. R. and T. J. Bennett (1980), "Analysis of the Low Frequency Ground Motion Environment For MX: Surface Waves and Valley Reverberation," Final Technical Report to Defense Nuclear Agency, DNA 5219F.

Murphy, J. R. (1981), "Near-Field Rayleigh Waves From Surface Explosions," Bull. Seism. Soc. Am., 71, p. 223.

Papoulis, A. (1962), The Fourier Integral and Its Applications, McGraw-Hill, New York.

Speicher, S. J. and H. L. Brode (1981), "Airblast Overpressure Analytic Expression For Burst Height, Range and Time-Over an Ideal Surface," Pacific-Sierra Research Corporation, Note 385, November.

DISTRIBUTION LIST

DEPARTMENT OF DEFENSE

Assistant to the Secretary of Defense
Atomic Energy
ATTN: Executive Assistant

Defense Advanced Rsch Proj Agency
ATTN: T. Bache

Defense Intelligence Agency
ATTN: DB-4C, E. O'Farrell
ATTN: DB-4N

Defense Nuclear Agency
2 cy ATTN: SPSS, G. Ullrich
4 cy ATTN: TITL

Defense Technical Information Center
12 cy ATTN: DD

Field Command
Defense Nuclear Agency, Det 1
Lawrence Livermore Lab
ATTN: FC-1

Field Command
Defense Nuclear Agency
ATTN: FCPR
ATTN: FCTX
ATTN: FCTT
ATTN: FCTT, G. Ganong
ATTN: FCTXE
ATTN: FCTT, W. Summa
ATTN: FCTK, C. Keller

Interservice Nuclear Weapons School
ATTN: TTV

Joint Strat Tgt Planning Staff
ATTN: NRI-STINFO Library
ATTN: JLA, Threat Applications Div

Under Secy of Def for Rsch & Engrg
ATTN: Strat & Theater Nuc Forces, B. Stephan
ATTN: Strategic & Space Sys (OS)

DEPARTMENT OF THE ARMY

BMD Advanced Technology Center
ATTN: 1CRDABH-X
ATTN: ATC-T

Chief of Engineers
Department of the Army
ATTN: DAEN-MPE-T
ATTN: DAEN-RDL

Harry Diamond Laboratories
ATTN: DELHD-NW-P
ATTN: DELHD-TA-L

US Army Ballistic Research Labs
ATTN: DRDAR-BLT, J. Keefer
ATTN: DRDAR-TSB-S

DEPARTMENT OF THE ARMY (Continued)

US Army Concepts Analysis Agency
ATTN: CSSA-ADL

US Army Engineer Ctr & Ft Belvoir
ATTN: DT-LRC

US Army Engineer Div Huntsville
ATTN: HNDED-SR

US Army Engineer Div Ohio River
ATTN: ORDAS-L

US Army Engr Waterways Exper Station
ATTN: J. Zelasko
ATTN: J. Strange
ATTN: J. Drake
ATTN: WESSE
ATTN: Library
ATTN: WESSA, W. Flathau
2 cy ATTN: WESSD, J. Jackson

US Army Material & Mechanics Rsch Ctr
ATTN: Technical Library

US Army Materiel Dev & Readiness Cmd
ATTN: DRXAM-TL

US Army Nuclear & Chemical Agency
ATTN: Library

USA Missile Command
ATTN: Documents Section

DEPARTMENT OF THE NAVY

Naval Civil Engineering Laboratory
ATTN: Code L51, J. Crawford

Naval Electronic Systems Command
ATTN: PME 117-21

Naval Facilities Engineering Command
ATTN: Code 04B

Naval Material Command
ATTN: MAT 08T-22

Naval Postgraduate School
ATTN: G. Lindsay
ATTN: Code 1424 Library

Naval Research Laboratory
ATTN: Code 2627

Naval Surface Weapons Center
ATTN: Code F31

Naval Surface Weapons Center
ATTN: Tech Library & Info Svcs Br

Naval War College
ATTN: Code E-11, Tech Service

DEPARTMENT OF THE NAVY (Continued)

Naval Weapons Evaluation Facility
ATTN: Code 10

Newport Laboratory
ATTN: Code EM, J. Kalinowski

Ofc of the Deputy Chief of Naval Ops
ATTN: OP 03EG
ATTN: NOP 981

Office of Naval Research
ATTN: Code 474, N. Perrone

Strategic Systems Project Office
ATTN: NSP-43

DEPARTMENT OF THE AIR FORCE

Air Force
ATTN: INT

Air Force Geophysics Laboratory
ATTN: LWH, H. Ossing

Air Force Institute of Technology
ATTN: Library

Air Force Office of Scientific Rsch
ATTN: W. Best
ATTN: J. Allen

Air Force Systems Command
ATTN: DLW

Air Force Weapons Laboratory
ATTN: SUL
ATTN: NTES, J. Thomas
ATTN: NTE, M. Plamondon
ATTN: NTES-C, R. Henny

Air University Library
ATTN: AUL-LSE

Ballistic Missile Office
ATTN: ENBF, D. Gage
ATTN: ENSN, A. Schenker
ATTN: EN

Deputy Chief of Staff
Logistics & Engineering
ATTN: LEEE

Deputy Chief of Staff
Research, Development & Acq
ATTN: AFRDQI

Foreign Technology Division
ATTN: NIIS Library

Rome Air Development Center
ATTN: TSLD

Strategic Air Command
ATTN: INT, E. Jacobsen
ATTN: NRI-STINFO Library

DEPARTMENT OF ENERGY

Albuquerque Operations Office
ATTN: R. Jones
ATTN: CTID

Nevada Operations Office
ATTN: Doc Con for Technical Library

OTHER GOVERNMENT AGENCIES

Central Intelligence Agency
ATTN: OSWR/NED

Department of the Interior
Bureau of Mines
ATTN: Tech Lib

NATO

NATO School (SHAPE)
ATTN: US Documents Officer

DEPARTMENT OF ENERGY CONTRACTORS

University of California
Lawrence Livermore National Lab
ATTN: D. Glenn
ATTN: Technical Info Dept Library

Los Alamos National Laboratory
ATTN: Reports Library
ATTN: J. Hopkins

Oak Ridge National Laboratory
ATTN: Civil Def Res Proj
ATTN: Central Rsch Library

Sandia National Lab
ATTN: Tech Lib, 3141
ATTN: Org 7112, A. Chabai
ATTN: L. Hill

Sandia National Labs, Livermore
ATTN: Library & Security Classification Div

DEPARTMENT OF DEFENSE CONTRACTORS

Aerospace Corp
ATTN: Technical Information Services

Agbabian Associates
ATTN: M. Agbabian

Applied Research Associates, Inc
ATTN: N. Higgins
ATTN: J. Bratton
ATTN: H. Auld

Applied Research Associates, Inc
ATTN: S. Blouin

Applied Research Associates, Inc
ATTN: D. Piepenburg

Applied Research Associates, Inc
ATTN: B. Frank

DEPARTMENT OF DEFENSE CONTRACTORS (Continued)

Applied Theory, Inc
2 cy ATTN: J. Trulio

AVCO Systems Division
ATTN: Library A830

BDM Corp
ATTN: T. Neighbors
ATTN: Corporate Library

BDM Corp
ATTN: F. Leech

Boeing Aerospace Co
ATTN: MS-85-20, D. Choate

Boeing Co
ATTN: Aerospace Library

California Institute of Technology
ATTN: T. Ahrens

California Research & Technology, Inc
ATTN: S. Schuster
ATTN: Library
ATTN: K. Kreyenhagen
ATTN: M. Rosenblatt

California Research & Technology, Inc
ATTN: D. Orphal

Calspan Corp
ATTN: Library

University of Denver
ATTN: Sec Officer for J. Wisotski

EG&G Wash Analytical Svcs Ctr, Inc
ATTN: Library

Electro-Mech Systems, Inc
ATTN: R. Shunk

Gard, Inc
ATTN: G. Neidhardt

Horizons Technology, Inc
ATTN: R. Kruger

IIT Research Institute
ATTN: M. Johnson
ATTN: R. Welch
ATTN: Documents Library

Institute for Defense Analyses
ATTN: Classified Library

Kaman AviDyne
ATTN: Library
ATTN: N. Hobbs

Kaman Sciences Corp
ATTN: Library

Kaman Tempo
ATTN: DASIAC

DEPARTMENT OF DEFENSE CONTRACTORS (Continued)

Lockheed Missiles & Space Co, Inc
ATTN: Technical Information Center
ATTN: T. Geers

Lockheed Missiles & Space Co, Inc
ATTN: J. Weisner, Dept 80-82

Martin Marietta Denver Aerospace
ATTN: D-6074, G. Freyer

McDonnell Douglas Corp
ATTN: R. Halprin

Merritt CASES, Inc
ATTN: Library
ATTN: J. Merritt

University of New Mexico
ATTN: N. Baum

Pacific-Sierra Research Corp
ATTN: H. Brode, Chairman SAGE

Patel Enterprises, Inc
ATTN: M. Patel

Physics International Co
ATTN: J. Thomsen
ATTN: F. Sauer
ATTN: E. Moore
ATTN: Technical Library
ATTN: L. Behrmann

R&D Associates
ATTN: R. Port
ATTN: J. Carpenter
ATTN: W. Wright
ATTN: Technical Information Center
ATTN: J. Lewis

R&D Associates
ATTN: H. Cooper

S-CUBED
ATTN: Library
ATTN: D. Grine
ATTN: T. Riney
ATTN: T. Cherry
4 cy ATTN: J. Murphy
4 cy ATTN: H. Shah
4 cy ATTN: T. Tzeng

S-CUBED
ATTN: J. Murphy

Science Applications, Inc
ATTN: Technical Library

Science Applications, Inc
ATTN: D. Maxwell
ATTN: D. Bernstein

Science Applications, Inc
ATTN: W. Layson

DEPARTMENT OF DEFENSE CONTRACTORS (Continued)

Southwest Research Institute
ATTN: A. Wenzel
ATTN: W. Baker

SRI International
ATTN: Y. Gupta
ATTN: D. Keough
ATTN: G. Abrahamson

Structural Mechanics Associates, Inc
ATTN: R. Kennedy

Teledyne Brown Engineering
ATTN: J. Ford
ATTN: F. Leopard
ATTN: D. Ormond

Terra Tek, Inc
ATTN: S. Green
ATTN: J. Schatz
ATTN: Library
ATTN: A. Abou-Sayed

DEPARTMENT OF DEFENSE CONTRACTORS (Continued)

Tetra Tech Systems Co
ATTN: L. Hwang

TRW Electronics & Defense Sector
ATTN: Technical Information Center
ATTN: P. Bhuta
ATTN: T. Mazzola
2 cy ATTN: N. Lipner

Universal Analytics, Inc
ATTN: E. Field

Weidlinger Assoc, Consulting Engrg
ATTN: M. Baron

Weidlinger Associates
ATTN: J. Isenberg

TRW Electronics & Defense Sector
ATTN: E. Wong
ATTN: P. Dai


FILM